Clim Dyn (2017) 49:1865–1883
DOI 10.1007/s00382-016-3421-z

The El Niño effect on Ethiopian summer rainfall

Stephanie Gleixner[1] · Noel Keenlyside[1,2] · Ellen Viste[1] · Diriba Korecha[3]

Received: 4 May 2016 / Accepted: 18 October 2016 / Published online: 3 November 2016

Abstract While El Niño is known to cause failure of Kiremt (boreal summer) rainfall in Ethiopia, the mechanisms are not fully understood. Here we use the ECHAM5 Atmospheric General Circulation Model to investigate the physical link between Pacific sea surface temperature (SST) anomalies and Kiremt rainfall. We compare ECHAM5 simulations forced with reconstructed SST data, to gauge-based rainfall observations and atmospheric reanalysis for the time period of 1961–2009. We perform composite analysis and sensitivity experiments driven only with equatorial Pacific SST anomalies. Our results show warm SST anomalies in the equatorial Pacific drive a corresponding large-scale circulation anomaly with subsidence over Ethiopia in dry Kiremt seasons. Horizontal wind fields show a slow-down of the whole Indian monsoon system with a weaker Tropical Easterly Jet and a weaker East African Low-Level Jet in these summers. These changes can be seen as an anomalous circulation cell over northern Africa with westerlies at 100–200 hPa and easterlies below 500 hPa. Surface easterlies might reduce the moisture inflow from the Atlantic and Congo basin into Ethiopia. This and the general subsidence over the region could explain the reduction in Kiremt rainfall. Our results suggest up to 50% of the Kiremt rainfall anomalies is driven by equatorial Pacific SST variability.

Keywords Ethiopia · Kiremt · ENSO · Walker-circulation

1 Introduction

Ethiopia is strongly dependent on agriculture, which supplies employment for 81% of the population and accounts for 40% of its gross domestic product (Äthiopien - Wirtschaft). Droughts and famines, such as the socio-economic catastrophe of 2011, call attention to the need for reliable seasonal forecasts for rainfall in this region to allow for agricultural planning and drought preparations. In this study we investigate the mechanisms of the predictability of Ethiopian summer rainfall associated with the influence of Pacific SST.

The operational seasonal forecasts of the National Meteorology Agency (NMA) of Ethiopia rely on an analogue method (Korecha and Sorteberg 2013b). The best three analogue years are chosen based on various oceanic and atmospheric patterns and indices. The main predictor is the current state and future development of ENSO indices. Numerous studies show correlation between Pacific SST and Ethiopian rainfall in all seasons (Beltrando and Camberlin 1993; Camberlin and Philippon 2002; Diro et al. 2008, 2011a; Gissila et al. 2004; Hansen et al. 2011; Korecha and Barnston 2007; Mutai et al. 1998; Segele et al. 2009a; Seleshi and Demaree 1995). However, the strength and sign of the correlation differ among seasons and regions.

The seasonal cycle of Ethiopian rainfall is dominated by the meridional migration of the Inter-Tropical Convergence Zone (ITCZ) across Ethiopia (Griffiths 1972; Segele et al. 2009a). While the south of Ethiopia experiences a bimodal rainfall cycle with rainy seasons in NH spring and autumn,

✉ Stephanie Gleixner
stephanie.gleixner@gfi.uib.no

[1] Geophysical Institute and Bjerknes Centre for Climate Research, University of Bergen, Postboks 7803, 5020 Bergen, Norway

[2] Nansen Environmental and Remote Sensing Center, Thormøhlens Gate 47, 5006 Bergen, Norway

[3] National Meteorology Agency for Ethiopia, Qelebet Menged, Addis Ababa, Ethiopia

central and northwestern Ethiopia has one main rainy season during NH summer (JJAS), called Kiremt. Overall, rainfall rates are highest during summer, with 65–95% of the All Ethiopian annual rainfall associated with Kiremt (Segele and Lamb 2005). This study focuses on Kiremt season only.

Generally, Kiremt rainfall and concurrent East Pacific SSTs show negative correlation and El-Niño years are associated with deficit rainfall (Beltrando and Camberlin 1993; Camberlin 2009; Diro et al. 2011a; Gissila et al. 2004; Korecha and Barnston 2007; Segele and Lamb 2005; Segele et al. 2009a; Seleshi and Demaree 1995; Tsegay 1997). Diro et al. (2011b) investigated the correlation between global SST and rainfall in different regions of Ethiopia. They show that JJAS summer rainfall in most of the country correlates negatively to an El-Niño-like SST pattern in the concurrent summer. Only the southeastern part of Ethiopia displays a weak positive correlation to equatorial East Pacific SST. Similarly, correlation between the JJAS Niño 3.4 index and rainfall over Ethiopia shows a clear dipole pattern with negative correlation in the northwestern part of the country and positive correlation in the southeast (Korecha and Barnston 2007). However, as Kiremt rainfall rates in southeast Ethiopia are low, All-Ethiopian summer rainfall is dominated by the northwest of the country and shows correlation between -0.7 and -0.8 with the Niño 3.4 index in the summer months (Korecha and Barnston 2007).

Although there is general agreement on a negative correlation between Pacific SST and Kiremt rainfall, to our knowledge only Diro et al. (2011b) showed evidence of a physical mechanism of a link between warm Pacific SST and a rainfall deficit in Ethiopia. Based on idealized SST-experiments with the Hadley Centre Atmosphere only GCM, they suggest two main mechanisms: an upper-level link via the Tropical Easterly Jet (TEJ) and a low-level link via the East African Low-Level Jet (EALLJ) and surface westerlies over North Africa.

In the upper troposphere, the TEJ forms during the May to September months. The core of the zonal jet is located between 100 and 200 hPa over the Indian subcontinent. JJAS average horizontal wind at 100 hPa shows the TEJ extending from the South China Sea to East Africa, with the highest wind speeds of around 30 m/s centered over southern India (Fig. 1a). Zonal jets induce a secondary meridional circulation at jet entrance (exit) to balance the acceleration (deceleration) of zonal geostrophic wind (Holton and Hakim 2013). Ethiopia is located southwest of the TEJ core (south of the jet exit) and according to this theory the jet induces upper-level divergence over Ethiopia. Observations show a divergence maximum at 100 hPa (Segele et al. 2009a). Upper-level divergence facilitates convection and therefore rainfall. This theory links the strength of the TEJ to Kiremt rainfall via vertical motion (Berhane et al. 2013; Camberlin 1997; Diro et al. 2011a; Segele and Lamb 2005; Segele et al. 2009a). Diro et al. (2011b) suggests that warm SST anomalies in the Central Pacific weaken the TEJ via upper-level Rossby waves and thereby weaken upper-level divergence over Ethiopia. This theory is supported by Shaman and Tziperman (2007), who show that NH summer El Niño events modify the TEJ via westward propagating upper-level Rossby waves and weaken the Indian summer monsoon rainfall, as the TEJ is the upper-level component of the Indian monsoon system.

In the lower troposphere, the EALLJ is the low-level component of the Indian monsoon system, therefore also peaking in NH summer. JJAS wind at 850 hPa shows the narrow meridional jet extending from east of Madagascar along the east coast of Africa and the Arabian Peninsula over the south of India (Fig. 1c). The strongest wind speeds exceed 20 m/s and are found along the Arabian Coast. The correlation of Ethiopian JJAS rainfall and EALLJ strength differs regionally. In southern Ethiopia the EALLJ is associated with surface divergence, and therefore suppressed rainfall. In North Ethiopia, which receives the bulk of Kiremt rainfall, rainfall is positively correlated with the EALLJ (Camberlin 2009; Diro et al. 2011a; Segele et al. 2009a, 2015). Diro et al. (2011b) find a weakening of the EALLJ in dry Kiremt seasons as well as in summers with warm east equatorial Pacific SST. In addition, Diro et al. (2011b) show that warm Pacific SST evoke low-level easterly wind anomalies over North Africa, which they proposed to be related to Kelvin wave propagation as part of a Gill response to the Pacific warming. These reduce the moisture influx from the Atlantic and Congo basin into the Ethiopia highlands, which is an important moisture source for the region (Diro et al. 2011b; Korecha and Barnston 2007; Mohamed et al. 2005; Segele et al. 2009a).

In addition to these two main mechanisms, Diro et al. (2011b) find southward shift of the African Easterly Jet (AEJ) related to warm SST anomalies in the Pacific and a Kiremt rainfall deficit. The AEJ is zonal jet at around 600 hPa (Fig. 1b). It extends over North Africa at about 15°N with a maximum over West Africa. However, this southward shift of the AEJ disagrees with the findings of Diro et al. (2011c), where a southward shift of the AEJ is associated with a strengthening of the AEJ and extra Kiremt rainfall in northeast Ethiopia during La-Niña-like conditions. The influence of Pacific SST on the AEJ, as well as the influence of the AEJ on Kiremt rainfall, is unclear.

So far, evidence of the physical mechanisms through which El-Niño-like SST anomalies in the Pacific influence Kiremt rainfall is limited to one model study and there is no complete theory. Therefore we further investigate the mechanisms with a different model and revisit the circulation changes that weaken Kiremt rainfall during warm Pacific episodes. We use the atmosphere general circulation

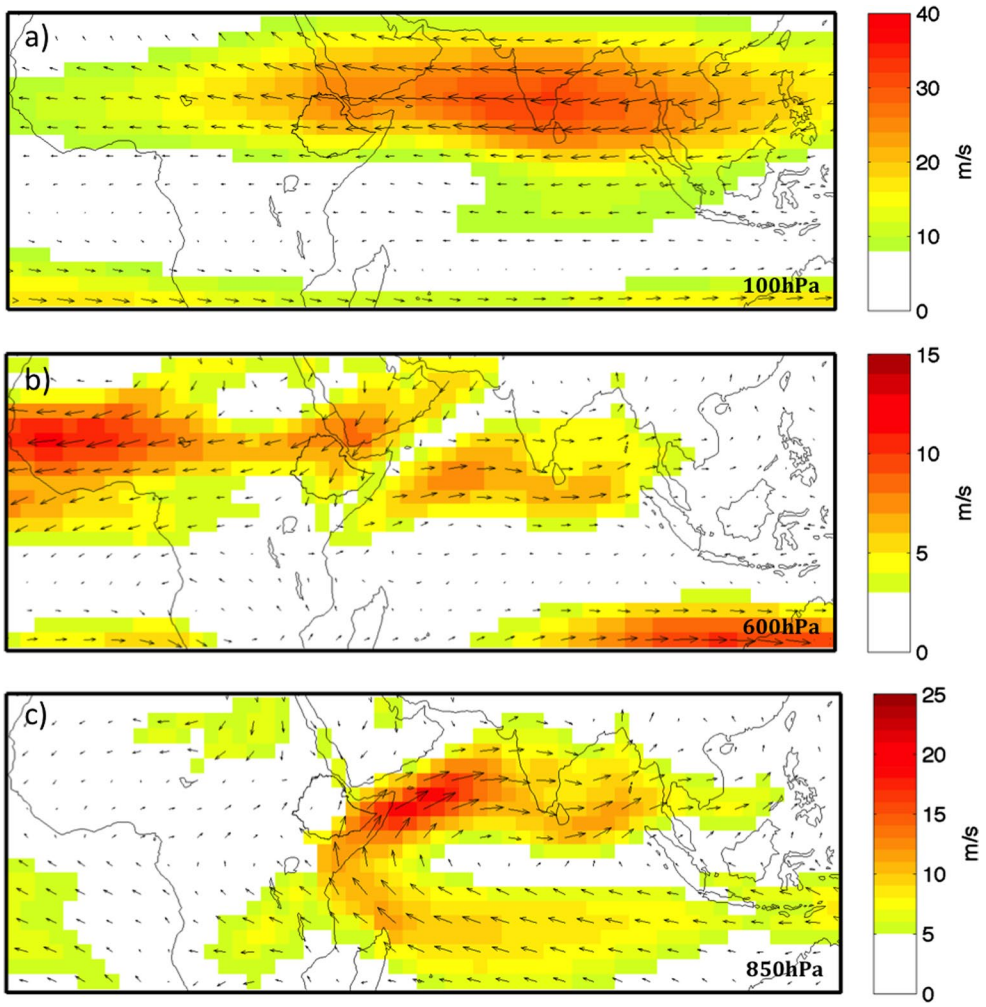

Fig. 1 JJAS mean horizontal wind speed (*colors*) in m/s and direction (*vectors*) at **a** 100 hPa, **b** 600 hPa and **c** 850 hPa averaged from 1961 to 2009 in JRA reanalysis

model (AGCM) ECHAM 5.3 to test the Kiremt response to El Niño-like SST anomalies in the Pacific Ocean. The following section describes the three data sets we used, the methodology of the composite analysis and the setup of the sensitivity experiment. In Sect. 3 we describe and discuss our results in four parts:

- Analysis of observational data sets shows the statistical relationship between Kiremt rainfall and Pacific SST.
- Model evaluation confirms that ECHAM5 captures the main features of rainfall in Ethiopia and of atmosphere variables related to Kiremt rainfall.
- Composite analysis of dry Ethiopian summers shows ECHAM5 can reproduce observed SST and associated circulation changes.
- A sensitivity experiment provides proof of causality and shows a physical link between Pacific SST anomalies and Kiremt rainfall.

A summary and conclusions are presented in a final section.

2 Data and methodology

2.1 Observed Ethiopian rainfall

We use two observational rainfall products of different spatial and temporal coverage, which we call Gstation (Grid points) and Zstation (Zones). Gstation is a set of monthly rainfall data from 1983 to 2010. This product is based on a blended rainfall data set, which combines interpolated in situ measurements from over 500 NMA rain gauges with satellite estimates (Dinku et al. 2014). The satellite data is TARCAT (TAMSAT African Rainfall Climatology And Time-series) version 2 from the TAMSAT (Tropical Applications of Meteorology using SATellite data

and ground-based observations) research group (Maidment et al. 2014). Dinku et al. (2014) provide a detailed description and evaluation of the data set. We use rainfall data at 717 grid points, which are unevenly distributed over Ethiopia and capture the wide range of inhomogeneous regions within the country. Because of the good spatial coverage and high quality of this data set we use it for the model evaluation. However, since it only has an overlap of 27 years with our ECHAM5 model data, we use a different product—Zstation—for the analysis of dry Ethiopian summers.

Zstation is a zone-based rainfall data set. Due to the inhomogeneity of precipitation over Ethiopia, several efforts have been made to divide Ethiopian into regions of homogenous rainfall (Diro et al. 2008, 2011b; Gissila et al. 2004; Korecha and Sorteberg 2013a). For Zstation Ethiopia was divided into 14 homogenous rainfall zones. Monthly rainfall anomalies were calculated from observations at 132 Ethiopian gauge stations of the NMA. For each zone anomalies of stations within the zone were averaged to get a rainfall time series for the zone. The detailed procedure is described in Viste et al. (2013). Here we use Zstation data for the time period from 1961 to 2009, which overlaps with the ECHAM5 historical simulations (see below).

2.2 Reanalysis and SST

We use Japanese 55-year Reanalysis (JRA-55, Kobayashi et al. 2015) as an observational estimate for atmospheric circulation variables. JRA-55 has a T319 horizontal resolution (~55 km) and 60 levels up to 0.1 hPa. Here we use horizontal wind and velocity potential for the time period from 1961 to 2009. For observed SST we use the Extended Reconstructed Sea Surface Temperature version 3b (ERSSTv3b) dataset, which is based on in situ measurements and available on a 2° grid. ERSSTv3b is ERSSTv3 (Smith et al. 2008) excluding satellite SST data that caused a cold bias.

2.3 ECHAM5 model simulations

This study focuses on the atmosphere model ECHAM5 (version 5.3) from the Max Planck Institute for Meteorology (Roeckner et al. 2003). This spectral model is used here with T106 (approximately 1°) horizontal resolution and 31 vertical levels extending up to 10 hPa (approximately 30 km). The convection parameterization is based on the Tiedke scheme (Tiedtke 1996). ECHAM5's good performance in the tropics is documented in numerous studies of tropical variability and predictability (Gleixner et al. 2014; Jiang et al. 2015; Mohino et al. 2011; Sperber et al. 2013). We use two types of ECHAM5 model runs: the first are historical simulations forced with observed SST for validation of the model and identification of rainfall related climate patterns. The second is an idealized sensitivity simulation forced with an El Niño-like SST pattern in the Tropical Pacific to investigate the causality and mechanisms that link Pacific SST and Ethiopian rainfall.

The historical simulations consist of a five-member ensemble driven with the ERSST monthly SSTs from 1870 to 2009 previously produced (Tseng 2012). These simulations include no time-varying external atmospheric forcing, and the ensemble members only differ in the initial 1870 SST conditions. For the dry Ethiopian summer composites we only use ECHAM5 data from 1961 onward, when Zstation data are available, and we use mainly the ensemble mean of 5 simulations.

The sensitivity simulation consists of a control run and a warm Pacific experiment. The control run is driven by the global SST monthly climatology for the period 1870–2009 computed from the ERSSTv3b. The model was run with this setup for 60 years, which we consider an equivalent of a 60-member ensemble of the climatological year. The warm Pacific experiment is based on the same setup as the control run, with the addition of positive SST anomalies in the equatorial East Pacific developing during months March to September. For a realistic SST pattern, we calculated monthly SST anomalies from the composites as described in the following section and added them to the SST climatology of the control run. January–February and September–December the model is forced with the same climatological SST as in the control run. The experiment run also covers 60 years with the identical SST pattern for every year. The atmospheric circulation adjusts to its basic state after September before the warm SST pattern in the East Pacific develops in March again. As we only investigate the summer months, we also consider the 60 years as 60 ensemble members of one-year long simulations forced with the same SST. The difference between these two experiments shows the impact of only the eastern equatorial Pacific SST anomalies. The significance of these differences is based on a student t test of means.

2.4 Dry Ethiopian summers

To identify large-scale climate variables linked to Kiremt rainfall, we use composite analysis based on precipitation. Here we focus on dry Ethiopian summers. We base the composites on the All-Ethiopian average rainfall during JJAS, while other studies limit Kiremt rainfall to Central-Northern Ethiopia (Segele and Lamb 2005; Segele et al. 2009a). However, since summer rainfall rates are low in the southeast of the country, the All-Ethiopian rainfall average is strongly dominated by rainfall rates in Central-Northern Ethiopia. We found no significant differences in the composites when using an All-Ethiopian rainfall time series in comparison to

a Central-Northern-Ethiopian time series. Therefore we use the All-Ethiopian rainfall time series to avoid choosing an arbitrary southern border for the Kiremt region.

We define dry summers by choosing Kiremt seasons with negative rainfall anomalies exceeding −1 standard deviation. To have a sufficiently long time series of Kiremt rainfall, we compare ECHAM5 to Zstation. For the model evaluation we consider the rainfall anomalies from 1961 to 2009. However, to construct the El Niño-like SST anomalies that force the sensitivity experiment, we make composites from the complete ECHAM5 time series from 1870 to 2009. We discuss this further in the results section.

We examine average climate conditions of ECHAM5 and Zstation dry summers in the ECHAM5 historical simulations and in the reanalysis, respectively. We focus on SST, wind and velocity potential. We calculate the composites by averaging over wind and velocity potential anomalies in the respective dry JJAS seasons. Anomalies are considered significant outside the 95% confidence level, which is defined as two standard deviations of the whole time series scaled by the square root of the number of composite members (Von Storch and Zwiers 2001).

3 Results and discussion

3.1 Observed rainfall data sets

Generally there is large uncertainty in Ethiopian rainfall in different observational data sets (Dinku et al. 2014; Otieno and Anyah 2013). We assume Gstation to be closest to reality and Zstation gives a very good approximation of the inter-annual variability of All-Ethiopian Kiremt rainfall, even though the spatial coverage of the rain gauges is much sparser. Although the variability of Zstation (standard deviation 0.5 from 1983 to 2009) overestimates the variability observed in Gstation (standard deviation 0.36 from 1983 to 2009), the two observational time series have a significant correlation coefficient of 0.95. Therefore we are confident to use Zstation as the observational rainfall data for the composite analysis and correlation analysis, which require a longer time series. Figure 2b shows the standardized All-Ethiopian JJAS in Gstation, Zstation and the ECHAM5 historical simulations from 1961 to 2009 (Gstation only 1983–2009) as well as the negative JJAS Niño 3.4 time series. There is a clear negative correlation between all three rainfall time series with the SST index. Zstation has a correlation of −0.71 with the JJAS Niño 3.4 time series. The strongest relationship between Pacific SST and Kiremt is found in summers of extreme SST. Table 1 shows the hit rates of the observed and simulated extreme Kiremt rainfall and the Nino3.4 extreme summers. In Zstation, there is a 75% likelihood of a dry Kiremt during warm SST in the Pacific (6 out of 8). During cold SST summers, 60% are wet Kiremt seasons in Zstation. There are no false hits in the observations (wet during warm SST or dry during cold SST).

3.2 Model evaluation

To ensure the suitability of ECHAM5 for an analysis of Kiremt rainfall we compare the seasonal cycle of rainfall in the ensemble mean of the ECHAM5 historical runs to Gstation, as its spatial coverage is much higher than Zstation. We regridded ECHAM5 and Gstation rainfall onto a 2.5 degree longitude-latitude grid to allow a comparison of the seasonal cycle for individual grid points over Ethiopia (Fig. 2a). ECHAM5 captures the strong regional differences in rainfall amounts and seasonality quite well. Both the model and observations show the clear distinction of the unimodal rainfall regime in the center and northwest of Ethiopia and the bimodal rainfall regime in the south and east of the country. In the southwestern part of Ethiopia ECHAM5 underestimates total rainfall amounts, while it tends to overestimate rainfall amounts in some of the central grid boxes, but the seasonality of rainfall agrees well with observations. As reference, Otieno and Anyah (2013) examined 10 CMIP5 coupled models for their representation of rainfall in the Horn of Africa and found that most models overestimate rainfall in the region and there are large differences in the meridional extent of the area associated with Kiremt rainfall.

ECHAM5 reproduces the observed relation to El Nino. Although it overestimates rainfall variance and underestimates the relationship to the equatorial Pacific SST in the individual runs, after ensemble averaging these two quantities are comparable to observations. The standard deviation of ECHAM5 ensemble mean JJAS rainfall in Ethiopia is 0.64 from 1983 to 2009 (the five ensemble members range from 0.74 to 0.84), which is comparable to Zstation. The correlation between Niño 3.4 and Kiremt rainfall in the ECHAM5 ensemble mean is −0.65 (the five ensemble members range from 0.46 to 0.58), which is closed to the observed correlation of −0.71. The hit rates of simulated extreme Kiremt rainfall and the Nino3.4 extreme summers (Table 1) show a 50% likelihood (4 out of 8) of a dry summer during warm Pacific conditions. Looking at all 5 ensemble members the likelihood of a dry summer during warm SST events is only 42%. Similarly, during cold SST summers, 50 and 56% are wet Kiremt seasons in the ECHAM5 ensemble mean and the ensemble members, respectively. ECHAM5 agrees well with observations in terms of false hits, with only one (two) wet Kiremt season during warm SST summers in the ensemble mean (the ensemble members) and no dry Kiremt during cold summers (Table 1). These results indicate a stronger influence of internal atmospheric variability and possibly also SST

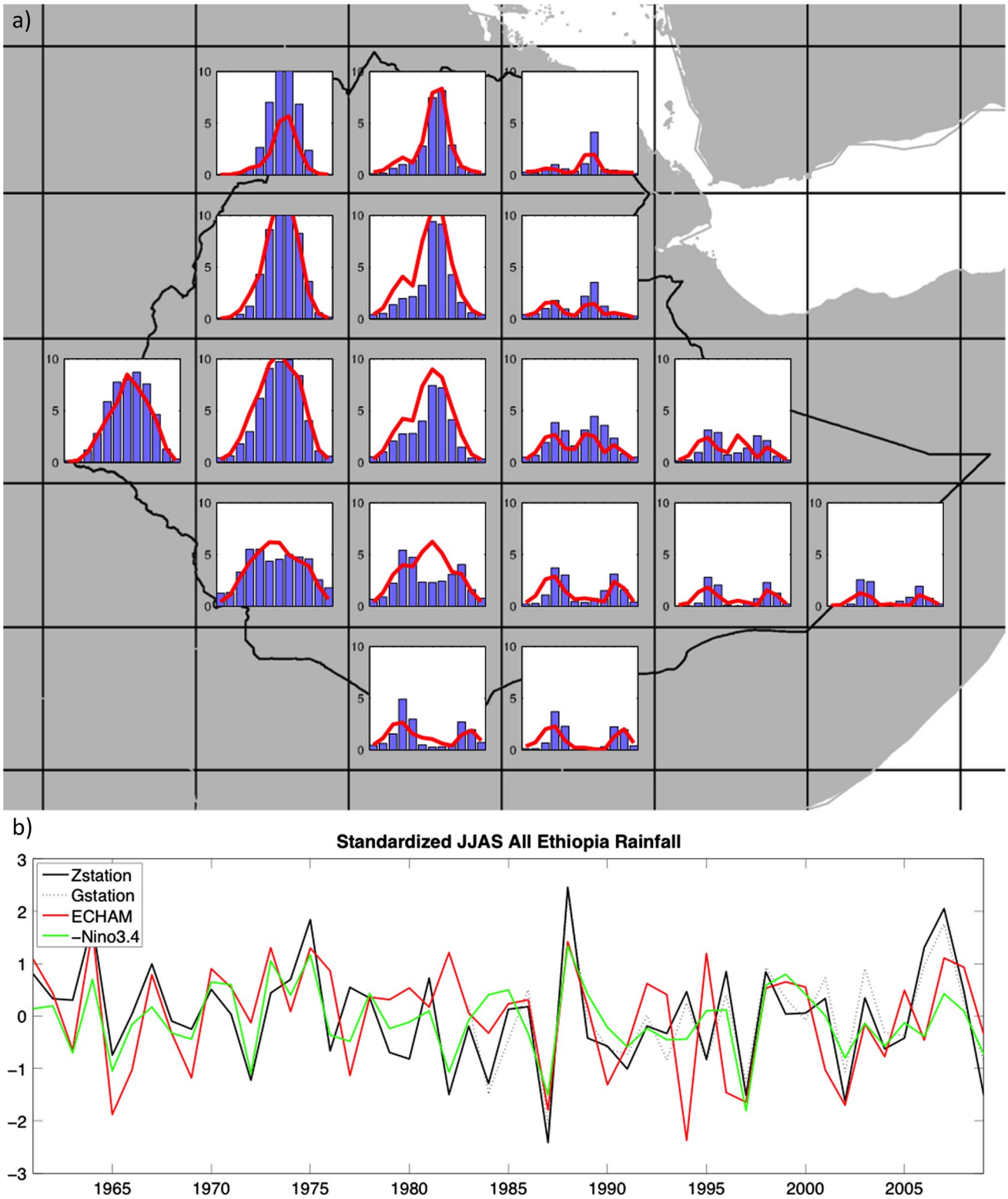

Fig. 2 **a** Monthly rainfall climatology of ECHAM5 (*red line*) and Gstation (*blue bars*) rainfall from 1983 to 2009 on a 2.5° grid over Ethiopia. Unit is mm/day. **b** Standardized average JJAS rainfall averaged over Ethiopia in Gstation (*black dotted*), Zstation (*black solid*) and ECHAM5 (*red solid*) in mm/day from 1961 (Gstation only from 1983) to 2009. The *green line* is the JJAS averages Niño 3.4 index from the NOAA website

Table 1 Number of years with JJAS Niño 3.4 above (warm) and below (cold) ±1 standard deviation, number of years with Ethiopian JJAS rainfall anomalies above (wet) and below (dry) ±1 standard deviation and number of years where warm/cold/wet/dry coincide in (a) Zstation, (b) ECHAM5 historical simulation ensemble mean and (c) the five ECHAM5 historical simulation ensemble members. The JJAS Niño 3.4 index is from the NOAA website

Nino3.4 index	Zstation 5 wet	Zstation 8 dry
8 warm	0	6
5 cold	3	0

Nino3.4 index	ECHAM5 mean 8 wet	ECHAM5 mean 11 dry
8 warm	1	4
5 cold	4	0

Nino3.4 index	ECHAM5 ensemble 41 wet	ECHAM5 ensemble 41 dry
40 warm	2	17
25 cold	14	0

from other regions on Ethiopian rainfall in the model. However, taking the ensemble mean reduces the importance of non-Pacific SST influences in warm/dry years. Overall we consider ECHAM5 a reasonable choice for this large-scale model study, as it captures the impact of ENSO variability on Kiremt rainfall quite well.

The correlation between simulated and observed Kiremt rainfall is significant and 0.43 and 0.45 with Zstation and Gstation, respectively. While these correlations may seem low, they are completely consistent with the assumption that the only SST influencing Kiremt rainfall are those in the equatorial Pacific and these explain around 50% of the variance ($r\sim = 0.7$); this can be shown by constructing a simple linear regression model between Nino3.4 SST and All Ethiopian Rainfall.

Since the influence of Pacific SST on Kiremt variability has been linked to changes in horizontal flow (Diro et al. 2011b), we examine the zonal and meridional winds field at the levels of the major jets over North Africa: the East African Low Level Jet (at 850 ha), the African Easterly Jet (600 hPa) and the Tropical Easterly Jet (100 hPa). Usually wind at 200 or 150 hPa is used to investigate the TEJ. However, Segele et al. (2009b) argues that the strongest upper-level divergence related to Ethiopian rainfall is located at 100 hPa, therefore wind changes at that level are of more interest.

Generally, ECHAM5 simulates the summer wind pattern in the African-Indian Ocean area very well, but with a slight overestimation of wind speeds in the major wind systems. At 100 hPa ECHAM5 underestimates wind speeds over Ethiopia (Fig. 3a). ECHAM5 simulates realistic core wind speeds of the TEJ, but the jet core over India and East Africa extends less to the south. Thus the TEJ may have a weaker connection with Ethiopian rainfall in ECHAM5 than in observations. At 600 hPa wind speed are weaker than in higher altitudes or at the surface (Fig. 1b). In JRA a northeasterly wind band over Yemen splits into a northerly and an easterly branch over Ethiopia. West of Ethiopia the easterlies stretch towards the Atlantic. The strongest easterlies, the AEJ over West Africa, reach maximum wind speeds between 10 and 15 m/s. ECHAM5 reproduces the overall pattern very well, but overestimates the easterly wind speeds at 600 hPa northwest of Ethiopia by up to 3 m/s, which corresponds up to a third of the mean flow in some regions (Fig. 3b). Comparatively large differences in 600 ha wind speed can be found in the western equatorial Indian Ocean, where ECHAM5 overestimates wind speeds by up to 8 m/s in comparison to JRA. At 850 hPa, except for the southeast, wind speeds within Ethiopia are very low, but it has to be considered that Central Ethiopia is mostly higher than 850 hPa (Fig. 1c). The difference in JJAS average wind speed between ECHAM5 and JRA at this level (Fig. 3c) show that model and observations agree well in the region of the EALLJ, with ECHAM5 overestimating the wind speed in the jet core by less than 5 m/s.

We use velocity potential at 200 hPa to characterize the large-scale circulation. Velocity potential describes the irrotational part of the flow. A positive velocity potential indicates large-scale convergence, which at 200 hPa can be related to sinking motion, while negative values indicate divergence and upward motion. The JJAS average velocity potential at 200 hPa is negative over south Asia and positive over the Atlantic and large parts of Africa (Fig. 4a). These features mark the zonal large-scale Walker-Circulation circulation. ECHAM5 captures this velocity potential pattern very well (Fig. 4b). In comparison to JRA reanalysis, the region of negative velocity potential extends further to the east. The difference between ECHAM5 and JRA JJAS velocity potential (Fig. 4c) shows that positive velocity potential is higher over Northern Africa and lower over South India in ECHAM5. Therefore the gradient of velocity potential over East Africa is sharper in ECHAM5; this could mean a stronger influence of velocity potential variations on Ethiopian rainfall in the model than in reality.

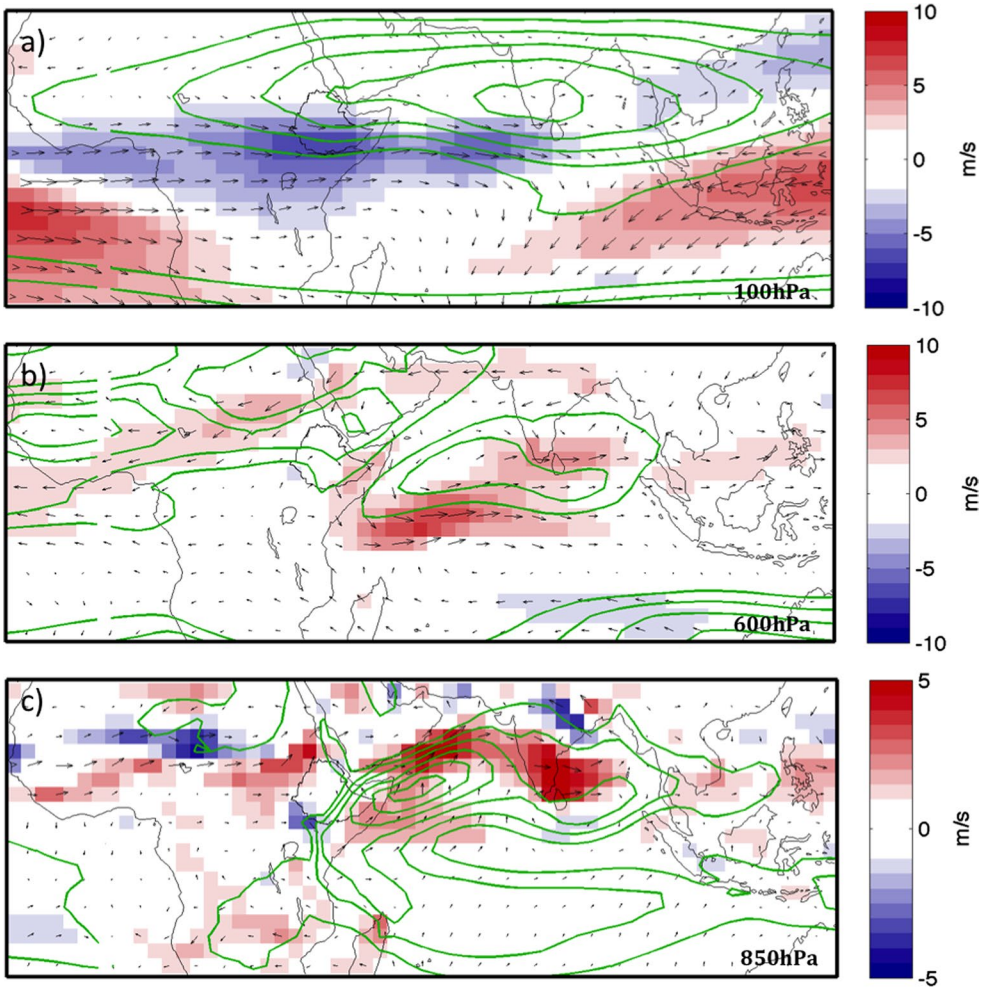

Fig. 3 *Colors* Difference between ECHAM5 historical runs and JRA reanalysis (ECHAM-JRA) in JJAS mean horizontal wind at **a** 100 hPa, **b** 600 hPa and **c** 850 hPa averaged from 1961 to 2009 in m/s. *Vectors* deviation of ECHAM5 wind vectors from JRA wind vectors over same time period. *Contours* same as Fig with *contours* in steps of **a** 5 m/s, **b** 2 m/s and **c** 2.5 m/s

3.3 Dry Ethiopian summers

The previous section showed that ECHAM5 simulates the average summer climate in the African–Indian Ocean regions reasonably well. Here we perform composite analysis using observed and simulated rainfall indices separately, as this identifies the processes responsible in the observations and the model without making any prior assumptions. The composite analysis shows the model's ability to capture observed circulation changes during dry Kiremt seasons, and identifies eastern Pacific SST as a key driver of these anomalies; the latter is confirmed in the next section for the model.

The eight and 11 dry summers that are identified in Zstation and ECHAM5, respectively (Table 1) are listed in Table 2. As to be expected from Table 1, the three years that are identified as dry summers in observations as well as in the model are also years of high JJAS Niño 3.4 indices. This level of agreement is consistent with the strength of the observed relation between Pacific SST and Ethiopian rainfall in JJAS.

The composite of rainfall anomalies in dry Kiremt seasons in Zstation shows that except for the very southeastern zone, all of Ethiopia is drier than average (Fig. 5a). The strongest rainfall anomalies are located in the northwest of Ethiopia with maximum anomalies around −1.5 mm/day. The anomaly distribution during dry Kiremt seasons in ECHAM5 (Fig. 6a) is similar, with dry conditions in all of Ethiopia except the southeast, and strongest anomalies in the northwest. Locally, rainfall anomalies in ECHAM5 reach values above 2 mm/day, but taking the higher horizontal resolution of the model data into account, the ECHAM5 anomalies agree very well with Zstation anomalies. The strongest differences between ECHAM5 and Zstation are in the southwest of Ethiopia, where ECHAM5 clearly overestimates rainfall anomalies. This is the region where ECHAM5 simulates a too strong seasonal cycle and generally overestimates JJAS rainfall (Fig. 2a). Therefore it is expected that anomalies in this region are stronger as well.

Consistent with previous studies (Diro et al. 2011b; Gissila et al. 2004; Segele et al. 2009a), SST

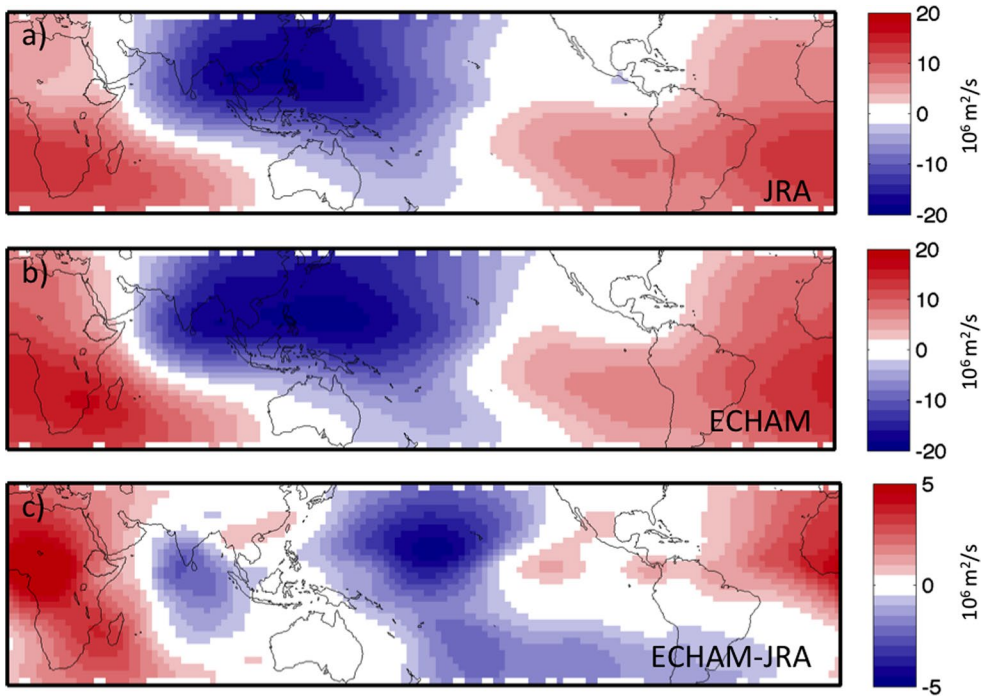

Fig. 4 JJAS velocity potential at 200 hPa, averaged from 1961 to 2009 in **a** JRA reanalysis and **b** the ECHAM5 historical simulations. **c** Difference between ECHAM5 historical runs and JRA reanalysis in JJAS velocity potential at 200 hPa from 1961 to 2009. Units are $10^6 m^2/s$

Table 2 Years with Ethiopian JJAS rainfall anomalies below −1 standard deviation as found in the ECHAM5 historical simulation and Zstation. The JJAS Niño 3.4 index is from the NOAA website

	1965	1966	1969	1972	1977	1982	1984	1987	1990	1991	1994	1996	1997	2001	2002	2009
ECHAM5																
Zstation																
Niño3.4	1	0.2	0.4	1.1	0.5	1.1	-0.4	1.5	0.2	0.6	0.4	-0.1	1.8	-0.01	0.8	0.7

anomalies in the dry Zstation summers show an El-Niño like pattern with warm SST anomalies in the Equatorial Pacific (Fig. 5b) up to 1.5 K. A recent study found the Indian Ocean, and to a lesser degree also the Atlantic, to have an influence on Kiremt variability (Segele et al. 2015), while in our composites significant SST anomalies are mostly limited to the Pacific Ocean.

ECHAM5 reproduces this observed relationship between Kiremt rainfall and SST very well. The SST composite based on dry summers in ECHAM5 (Fig. 6b) also shows significant warm anomalies in the equatorial Pacific, albeit weaker and only in the central Pacific. However, when using the whole ECHAM5 run from 1870 to 2009 for the composite, as done to find the SST anomaly pattern for the sensitivity runs, 20 dry Kiremt seasons are identified and the corresponding SST pattern extends to the west coast of South America, matching the observations very well (see next section). In our linear analysis we find little evidence of SST in other regions contributing to Ethiopian rainfall variability in this season.

The large-scale circulation anomalies in the eight observed dry Kiremt seasons are represented by velocity potential anomalies at 200 hPa (Fig. 5c). Negative anomalies over the equatorial central and eastern Pacific and positive anomalies over the Indian Ocean and East Africa indicate a Walker-Cell like response to the SST pattern with upward anomalies over the warm SST in the Pacific and balancing downward anomalies over the whole Indian Ocean. This pattern already indicates that there are westerly wind anomalies in upper levels over Africa. ECHAM5 shows a very similar circulation anomaly in dry Kiremt seasons, but the cell is slightly shifted to the west (Fig. 6c), consistent with the corresponding SST anomalies in the same summers. The positive (downward) velocity potential anomalies directly over Ethiopia indicate a direct effect of the cell-like circulation anomaly on Kiremt rainfall via the suppression of convection, similar to subsidence anomalies

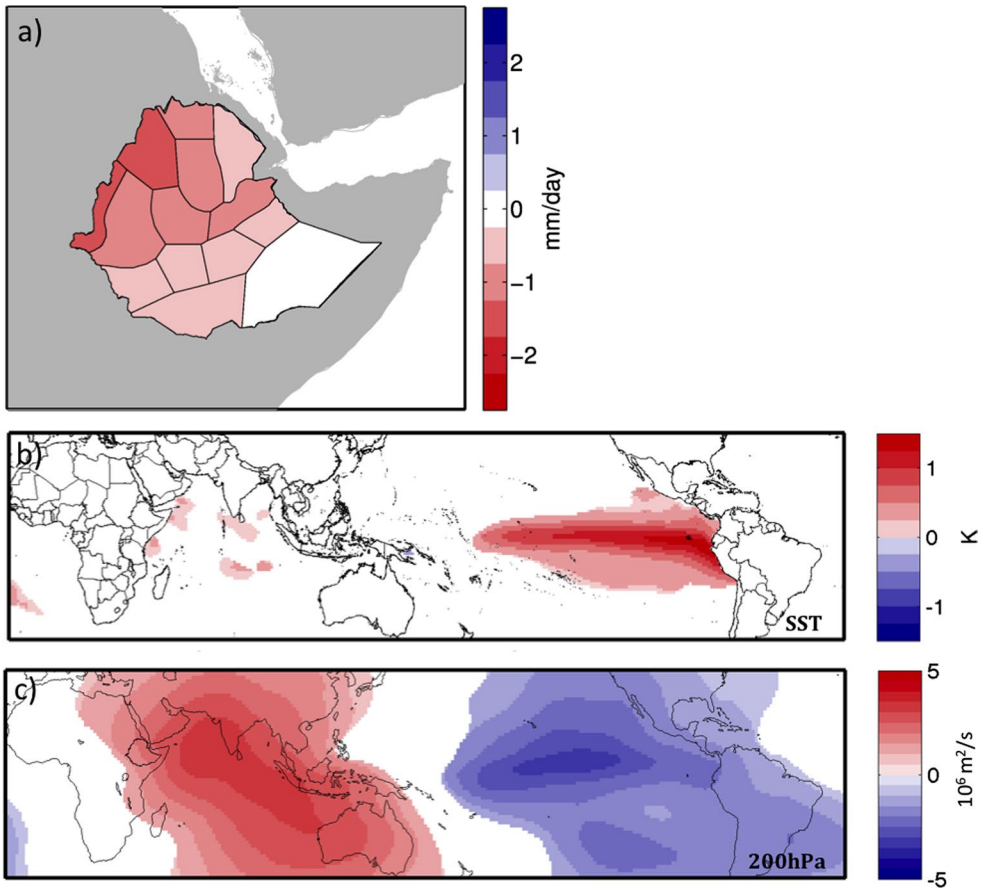

Fig. 5 Composites based on 8 dry Ethiopian summers in Zstation 1961–2009: **a** observed JJAS rainfall anomalies in the 14 zones of Zstation in mm/day, **b** observed, significant (95% level) JJAS SST anomalies from ERSST3vb in Kelvin and **c** significant (95% level) JRA velocity potential anomalies at 200 hPa in 10^6 m^2/s

found in another model study (Diro et al. 2011b). In contrast to the SST anomalies, the velocity potential anomalies are stronger in ECHAM5 than in the observations. This is consistent with the simulated mean state, which suggests the role of the velocity potential might be overestimated in ECHAM5.

The mechanisms proposed by Diro et al. (2011b) to connect Pacific SST and Kiremt rainfall—namely the weakening of the TEJ and EALLJ—is seen in composites of the horizontal wind fields. Colours in the wind anomaly composite figures show the strength of the anomalous wind, not the anomalous wind speed, in order to take the direction of the wind anomalies into account. In dry Ethiopian summers, observations and ECHAM5 show significant westerly wind anomalies at 100 hPa over all of North Africa (Figs. 7a, 8a). This means a weakening of the wind speeds in the TEJ exit region, and supports the idea of the upper-level link between Pacific SST and Kiremt rainfall via a weakening of the TEJ. The location of the positive velocity potential anomalies in upper levels over the Indian Ocean (Figs. 5c, 6c) is related to these wind anomalies, representing the large-scale convergent anomaly given by westerly anomalies over Northern Africa. In addition, the weakening of the TEJ over Ethiopia indicates a weakening of the meridional secondary circulation and therefore the upper-level divergent flow, suppressing upward motion, convection and rainfall. As with the composite SST anomalies, the composite 100 hPa wind anomalies are stronger in the observations than in ECHAM5.

In the mid-troposphere easterly anomalies prevail in dry summers. In reanalysis, composites of horizontal wind at 600 hPa in dry summers (Fig. 7b) show significant easterly anomalies over equatorial West Africa, indicating a strengthening and southward shift of the AEJ. These results support findings of Diro et al. (2011b) and disagree with the findings of Diro et al. (2011c), who find an acceleration and southward drift of the AEJ in NH summers of excess precipitation in the northwest of Ethiopia. Over Ethiopia there are weak easterly anomalies in the mid-troposphere. In ECHAM5 (Fig. 8b), there are significant easterly anomalies over all of Central Africa during dry summers, with maximum anomalies of up to 4 m/s over the Horn of Africa, where average wind speeds are less than 10 m/s (Figs. 1b, 3b). These mid-level easterly anomalies are part of a larger cell and contribute to the return flow of the upper level westerlies.

The low-level link between Pacific SST and Kiremt rainfall via the EALLJ is hinted at in the composites of

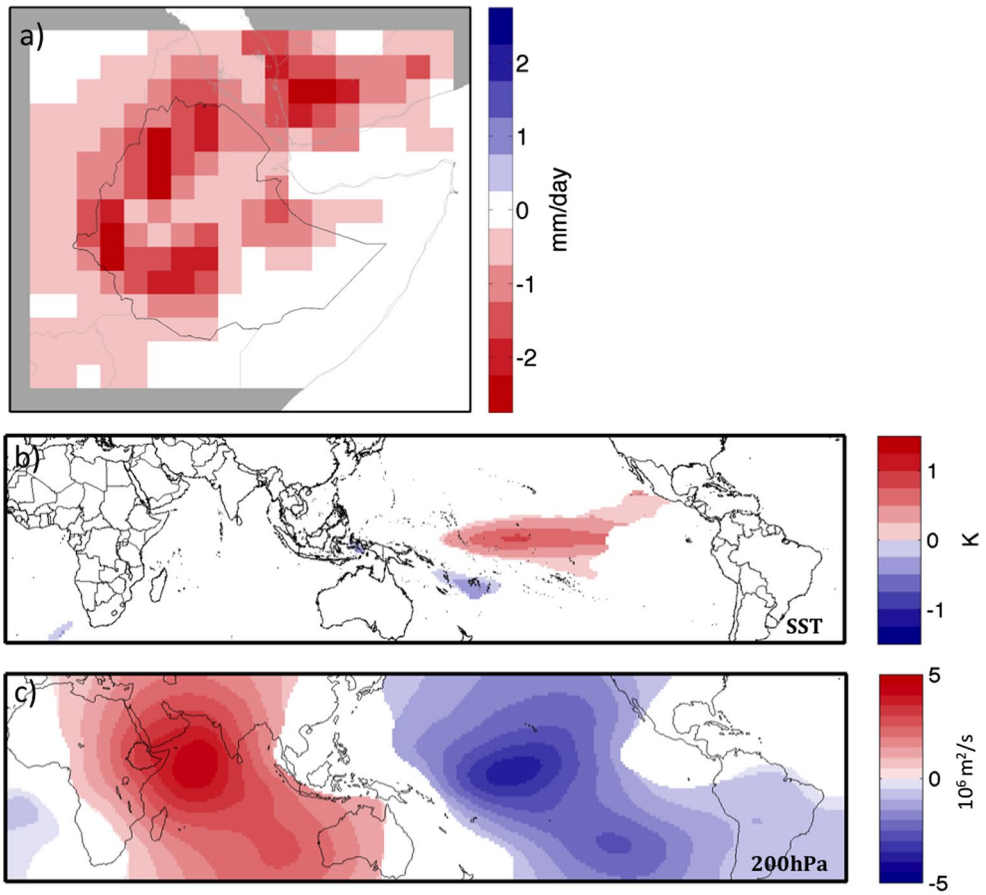

Fig. 6 Composites based on 11 dry Ethiopian summers in the ECHAM5 historic simulation 1961–2009: **a** simulated JJAS rainfall anomalies in mm/day, **b** observed, significant (95% level) JJAS SST anomalies from ERSST3vb in Kelvin and **c** significant (95% level) simulated velocity potential anomalies at 200 hPa in 10^6 m^2/s

horizontal wind at 850 hPa. In dry summers, the reanalysis shows northeasterly anomalies along the East African coast and therefore a weakening of the EALLJ (Fig. 7c). In ECHAM5, the low-level wind anomalies in dry summers are easterly over central Africa and off the coast of the Horn of Africa (Fig. 9c). This contributes to a weakening of the EALLJ over the Arabian Sea, but seems to be part of the overall signal of anomalous low-level flow from the Indian Ocean to the Atlantic Ocean, which has also been shown in Diro et al. (2011b). In both, observations and ECHAM5, there are easterly and northeasterly anomalies west of Ethiopia in dry summers. These wind anomalies would reduce the inflow of moisture from the west into northern and central Ethiopia. Viste and Sorteberg (2013) showed that the moisture transport branches from the Atlantic, Indian Ocean and central Africa, which enter Ethiopia from the west, weaken during dry summer months.

The reanalysis wind anomalies in dry Ethiopian summer composites can be interpreted as an overall weakening of the Indian monsoon system, with a weak TEJ at the upper-level and a weak EALLJ near the surface. The circulation anomalies in the ECHAM5 composites are more zonal in nature and give a picture of a large-scale cell with westerly anomalies in the upper-levels and easterly anomalies in the middle troposphere. Nonetheless, these composite results show that ECHAM5 can reproduce observed circulation changes during dry Kiremt seasons that have been known from previous studies. These results support ECHAM5 as a choice for investigating the mechanism of the influence of Pacific SST and Kiremt. In the next section, sensitivity experiments isolate the impact of tropical Pacific SST and demonstrate a causal link.

3.4 Warm Pacific experiment

We perform two additional experiments that differ only by a warm SST anomaly that is prescribed in the tropical Pacific. As explained in the Data and Method section, this Warm Pacific experiment is set up with developing warm SST anomalies as identified in dry JJAS composites. In contrast to the previously examined composites, we use the whole time series from 1870 to 2009 to identify 20 dry summers to composite the monthly SST anomalies used in this sensitivity experiment. The longer period allows a more robust determination of the driving SST pattern, which shows some marked differences between observations and model when computed from the shorter observational period (see previous section). Figure 9 shows the

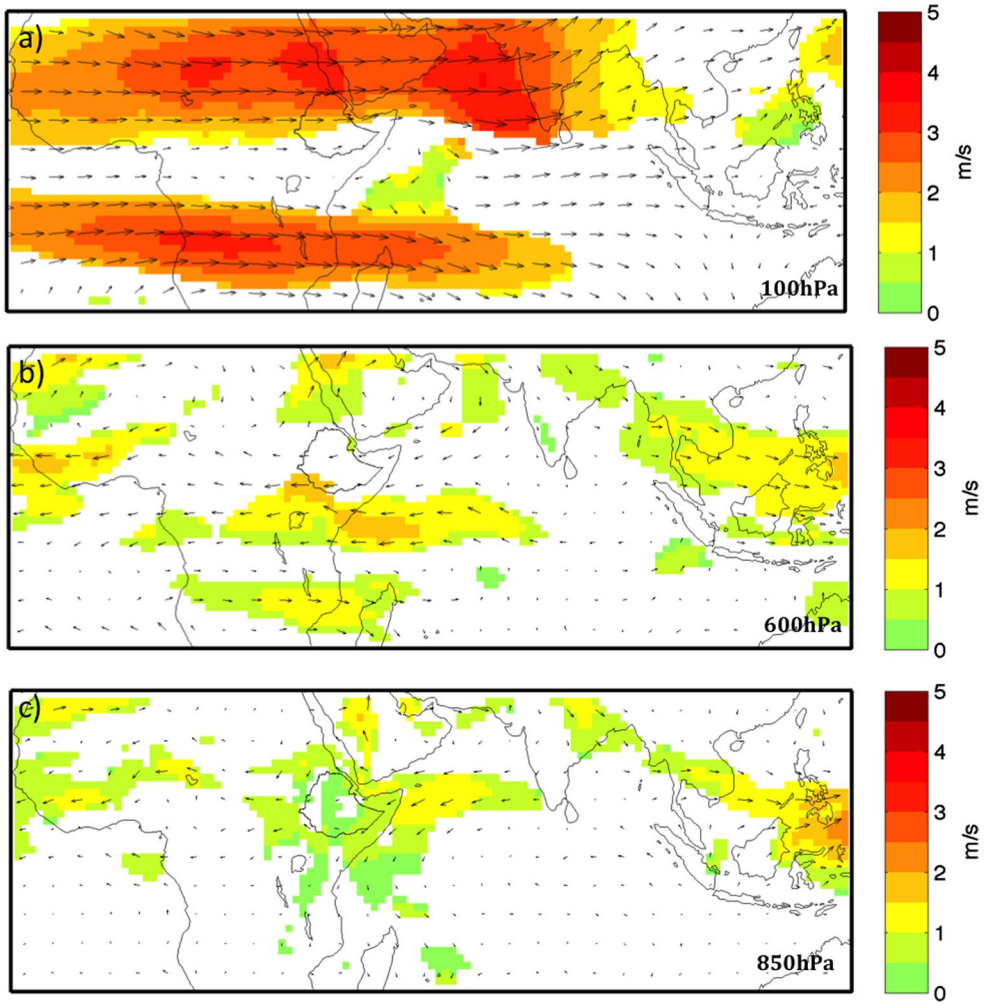

Fig. 7 Composites based on 8 dry Ethiopian summers in Zstation 1961–2009: significant (95% level) JRA JJAS wind anomalies in vectors at **a** 100 hPa, **b** 600 hPa and **c** 850 hPa. *Colours* show the strength of the anomalous wind, units are m/s

monthly SST differences between the control run, which is forced with climatological ERSST, and the Warm Pacific experiment. We prescribed the SST anomalies from March to September for the Pacific only, which corresponds to a developing El Niño. The results of this experiment are shown as the difference to the Control run. In order to ensure statistically robust results both experiments are 60 years long.

The rainfall response in the Warm Pacific experiment shows that positive SST anomalies in the central and eastern Pacific cause reduced Kiremt rainfall (Fig. 10a). JJAS rainfall anomalies in the sensitivity experiment are significantly lower than in the Control with a band of rainfall deficit from south Sudan into Yemen with a maximum signal of up to −2.5 mm/day over northern and western Ethiopia. ECHAM5 computes rainfall in the convection scheme (convective rainfall) and in the cloud scheme (large-scale rainfall). The comparison of the two types of rainfall (Fig. 10b, c) shows that the negative rainfall anomalies over Ethiopia are due to a decrease of the large-scale rainfall. In contrast, the convective rainfall is slightly stronger in the Warm Pacific experiment than in the Control. Surface heating appears to drive increased convection. The difference between the Warm Pacific experiment and the Control in JJAS surface temperature shows a surface warming over large areas of North Africa with strongest warm anomalies of about 1.5 K around northern Ethiopia (Fig. 11a).

The difference in velocity potential at 200 hPa between the Warm Pacific experiment and the Control in JJAS (Fig. 11b) is positive over the Indian Ocean and East Africa and negative over the Pacific Ocean. The pattern and amplitude look strikingly similar to the JJAS composite of dry summers in ECHAM5 (Fig. 6c), but slightly eastward shifted consistent with the corresponding SST pattern differences. We can now directly attribute this zonal circulation anomaly, that induces sinking and therefore suppression of

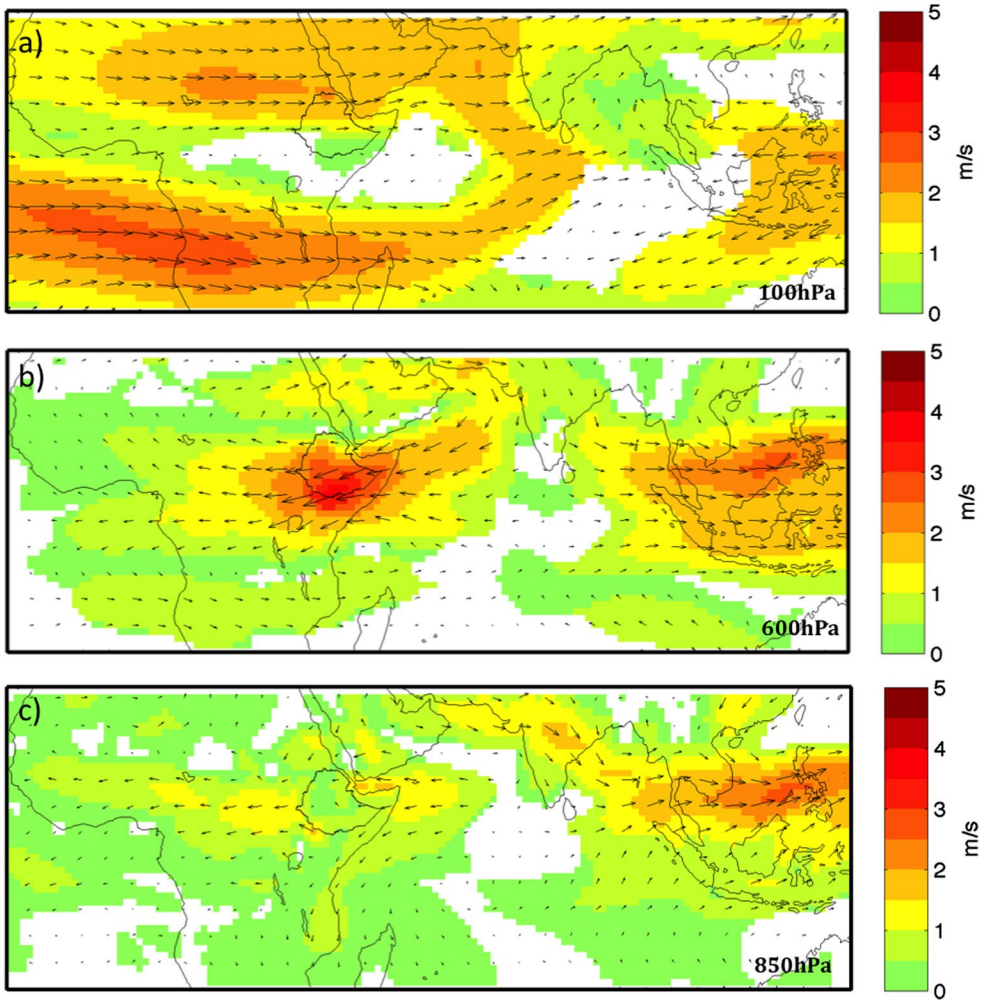

Fig. 8 Composites based on 11 dry Ethiopian summers in the ECHAM5 historic simulations 1961–2009: significant (95% level) simulated JJAS wind anomalies in vectors at **a** 100 hPa, **b** 600 hPa and **c** 850 hPa. *Colours* show the strength of the anomalous wind, units are m/s

rainfall over Ethiopia, to the warm SST anomalies in the Pacific. The overall sinking motion over Ethiopia explains the strong signal in large-scale precipitation.

To obtain a clearer picture of this cell-like anomaly pattern we examine a cross-section over the latitude band from 0° to 20°N, to capture the response over Ethiopia as well as the local response to the equatorial SST warming pattern in the Pacific (Figs. 12, 13). As precipitation changes are related to either circulation or moisture changes, we investigate both in these figures. The vectors show horizontal and vertical wind on 27 levels. Colors show the horizontal moisture convergence on the same levels. Moisture convergence is calculated from the seasonal means of wind and specific humidity, in order to allow for comparison of the mean changes of two components in moisture convergence between the two model runs (see below). Since large-scale variability dominates moisture transport in the tropics (Peixoto 1992), moisture convergence can be calculated from data beyond the synoptic scale (Chakraborty et al. 2006). The topography is approximated by surface pressure at 10°N in black shading, which shows the plateau in central Ethiopia as the highest elevation at this latitude.

The difference between the Warm Pacific experiment and the Control in horizontal moisture convergence (Fig. 12) shows the typical El Niño response with low-level moisture convergence and upward motion in the west of the SST anomaly pattern, in agreement with the negative upper-level velocity potential over the central Pacific. Subsidence balancing this upward branch is found to the east (over the eastern Pacific) and to the west (over the Indian Ocean) of the region of upward motion. This corresponds to a weakening of the TEJ jet over Africa, west of the velocity potential anomaly maximum, but not at its core over India. The strongest sinking signal is located over the western Indian Ocean and extends into the African continent. However, the vertical motion response directly over Ethiopia is rather inhomogeneous and includes upward motion over the Ethiopian highlands. This agrees with the increase of convective precipitation in the region (Fig. 10b). On the other hand, over Ethiopia moisture divergence dominates

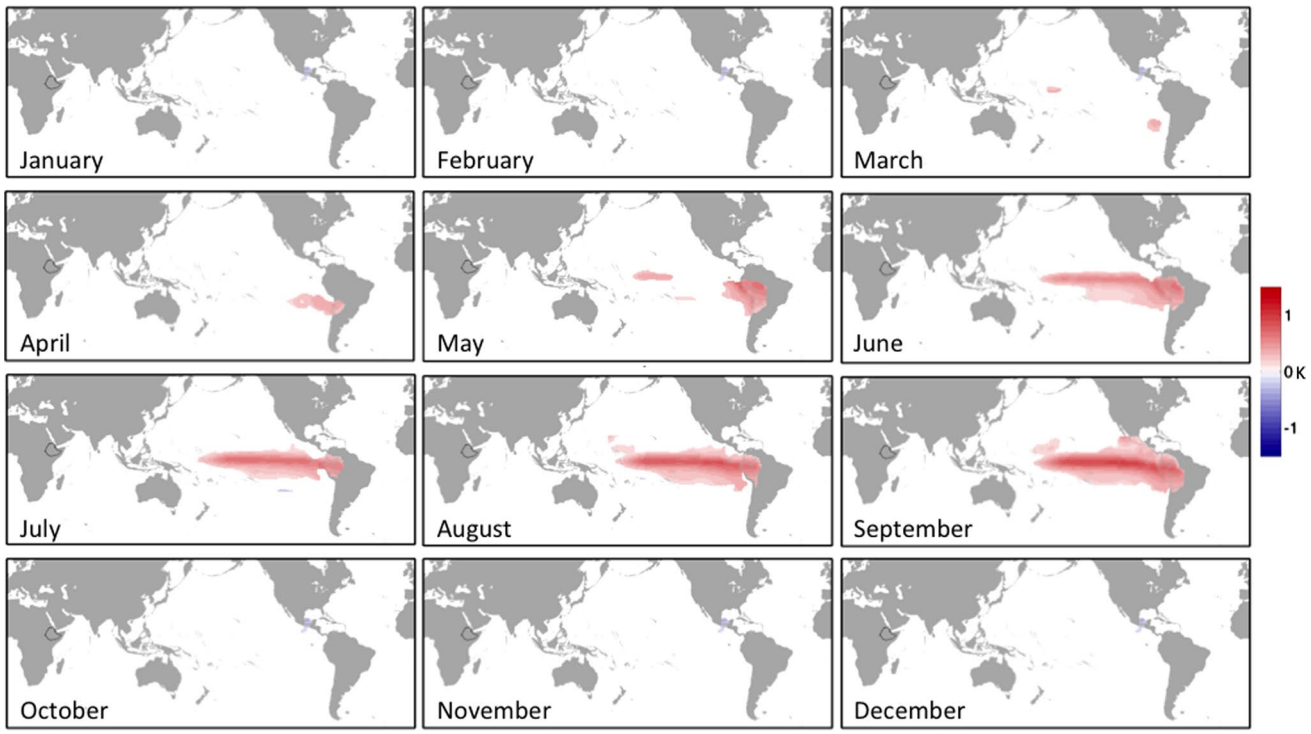

Fig. 9 Composites based on 20 dry Ethiopian summers in the ECHAM5 historical simulations 1870–2009: significant (95% level) observed monthly ERSST3vb SST anomalies from March to September in Kelvin as used to force the warm Pacific experiment

from the surface up to 400 hPa, in agreement with the overall reduction in rainfall (Fig. 10a).

The change in horizontal moisture convergence can be separated into three terms:

$$\Delta\left(-\nabla\cdot\left(\vec{v}\times q\right)\right)=-\nabla\cdot\left(\Delta\vec{v}\times q\right)-\nabla\cdot\left(\vec{v}\times\Delta q\right)-\nabla\cdot\left(\Delta\vec{v}\times\Delta q\right)$$

We are interested in the impact of circulation changes versus moisture changes, therefore we compare the first two terms on the right hand side: the divergence resulting from change in wind (i.e. Warm Pacific minus Control) but no change in specific humidity (i.e. Control) (Fig. 13a) and the divergence resulting from change in specific humidity but no change in wind (Fig. 13b). The third term that results from changes in both (i.e. excluding the background) is found to be negligible. Comparing the two first terms clearly shows the dominating impact of circulation changes. The divergence of wind change and control specific humidity (Fig. 13a) closely resembles the total horizontal moisture convergence change (Fig. 12) in pattern and magnitude.

The overall sinking motion over the Indian Ocean and East Africa seems to be balanced by lower level westerly anomalies over the Pacific and easterly anomalies over central Africa (Fig. 12). These easterly anomalies over Africa extend up to 500 hPa. The horizontal wind field at 600 hPa (not shown) resembles closely the composite of 600 hPa winds in dry Kiremt summer in ECHAM5 (Fig. 8b). These strong easterly anomalies in the middle troposphere are consistently related to dry Kiremt in ECHAM5 and may affect rainfall by an increase of moisture transport from Ethiopia. Low-level easterlies could explain a reduction in rainfall via a decrease in moisture inflow from the west, but cannot be related to changes in the EALLJ.

This simulation gives consistent picture of the circulation and moisture changes during warm Pacific/dry Kiremt episodes. To obtain a comparable picture in observations, we did a composite of seven JJAS seasons from 1961 to 2009, based on Niño3.4 index exceeding one standard deviation. The observational composite is limited to this period by rainfall data availability. Model composites are based on the same seven events, as ECHAM5 is driven by observed SST. Rainfall, wind and velocity potential anomalies in these composite (not shown) strongly resemble the dry Kiremt composite anomalies (Figs. 5, 6, 7, 8). The cross-section of 0°–20°N of observed anomalies in this composite agrees very well with the sensitivity experiments (Fig. 14). The horizontal moisture convergence anomalies over Ethiopia are mainly negative. The zonal and vertical wind anomalies display the same large-scale cell as in the sensitivity experiment. However, the vertical motion over Ethiopia is uniformly downward, therefore giving a clearer indication of suppressed rainfall.

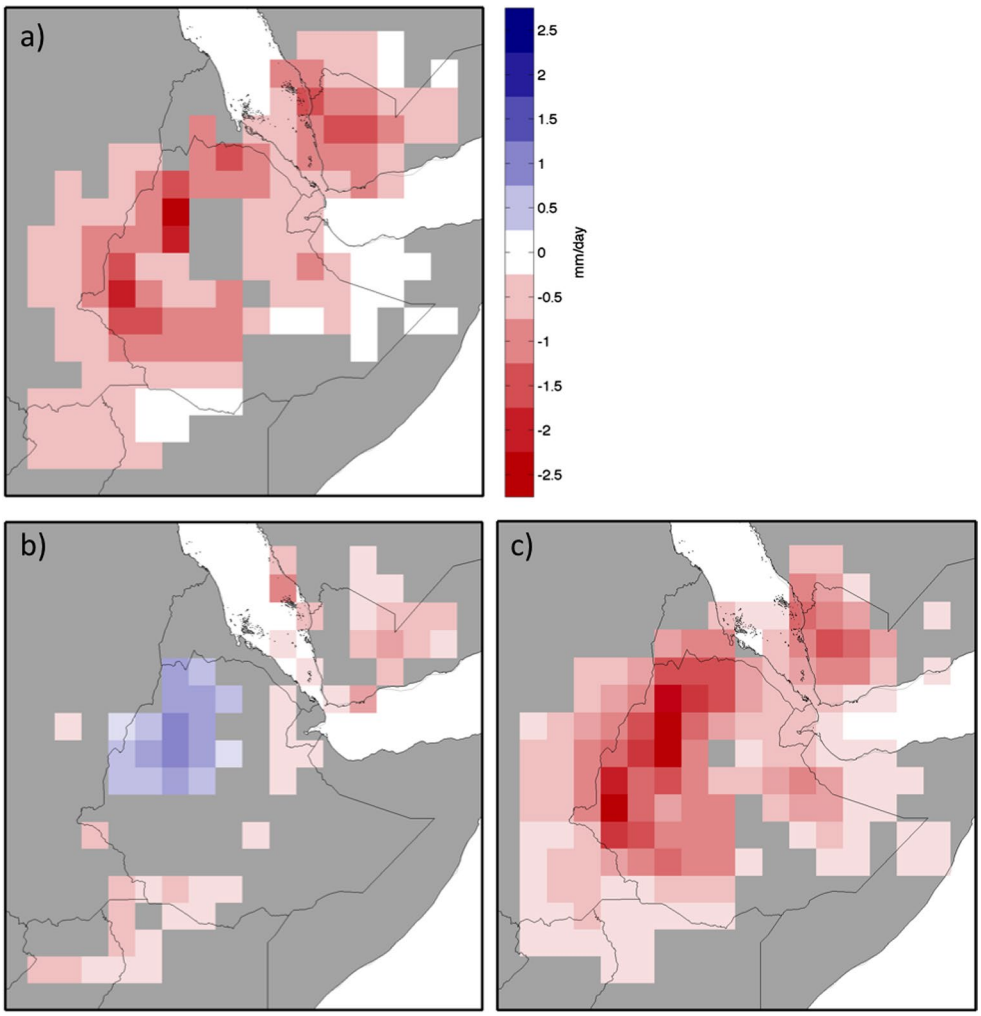

Fig. 10 Significant (99% level) difference in **a** total precipitation, **b** convective precipitation and **c** large-scale precipitation between ECHAM5 Warm Pacific experiment and Control in Kiremt (JJAS) in mm/day over the Horn of Africa

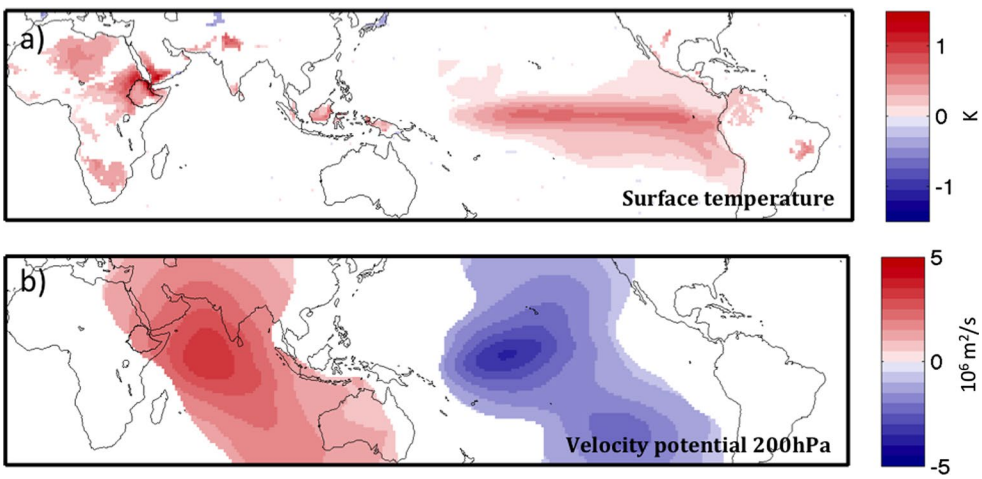

Fig. 11 Significant (99% level) difference in **a** velocity potential at 200 hPa in 10^6 m^2/s and **b** surface temperature in Kelvin between ECHAM5 Warm Pacific experiment and Control in JJAS (Warm Pacific–Control)

4 Summary and conclusion

We have used observations, atmospheric reanalysis and the atmosphere model ECHAM5 to investigate the connection between dry summers in Ethiopia and warm SST in the Pacific Ocean.

Comparison to observations show ECHAM5 is suitable to study the influence of SST on to Kiremt rainfall. In

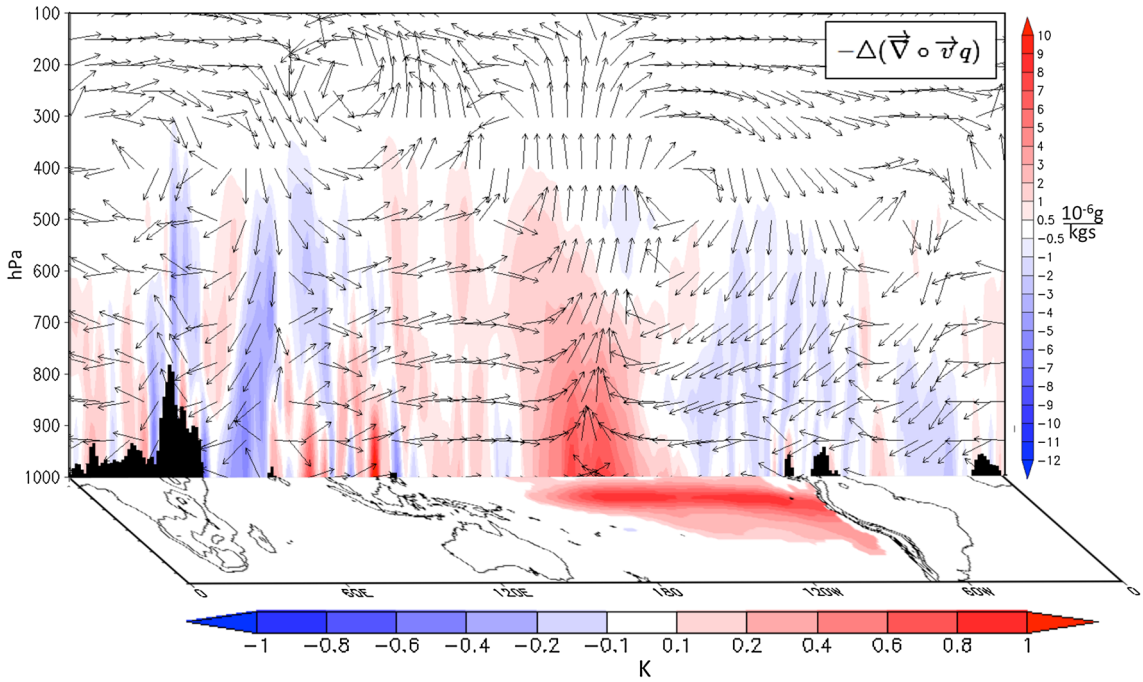

Fig. 12 Difference between ECHAM5 Warm Pacific experiment and Control in JJAS. The *upper panel* vectors show vertical and zonal wind speed differences averaged from 0 to 20 N. In the horizontal only every 5th vector is shown. *Colours* are the difference in horizontal moisture convergence in g/kgs on 27 pressure levels. The *lower panel* shows the SST anomalies that force the model, it is identical to the JJAS SST average from Fig. 9

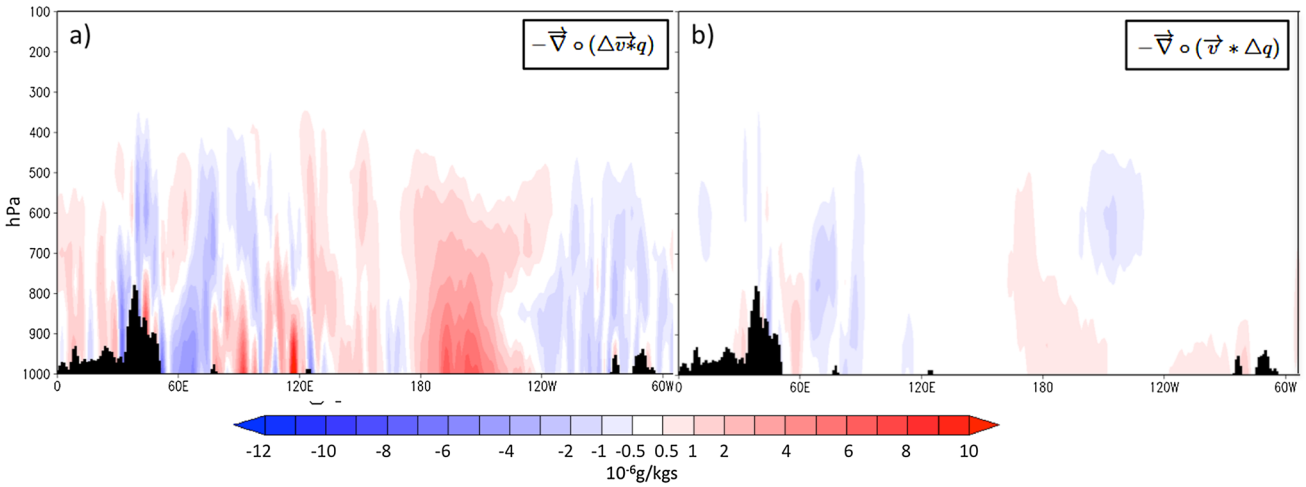

Fig. 13 Difference between ECHAM5 Warm Pacific experiment and Control in JJAS. *Colours* are the difference in two terms of the horizontal moisture convergence in g/kgs on 27 pressure levels: **a** convergence of control specific moisture multiplied with the horizontal wind difference between ECHAM5 Warm Pacific experiment and control. **b** Convergence of horizontal wind multiplied with the specific moisture difference between ECHAM5 Warm Pacific experiment and control

particular, ECHAM5 captures the rainfall amounts and variability of Kiremt reasonably well when driven with historical SST. The relative importance of variability related to Pacific SST appears to be underestimated in the individual ensemble runs. However, the observed relations are revealed in the ensemble average and the impact of ENSO variability on Kiremt variability in ECHAM5 matches observations well in terms of strength and pattern. As the observations, ECHAM5 shows that during dry Ethiopian summers Pacific SSTs tend to be significantly warmer than average. ECHAM5 also

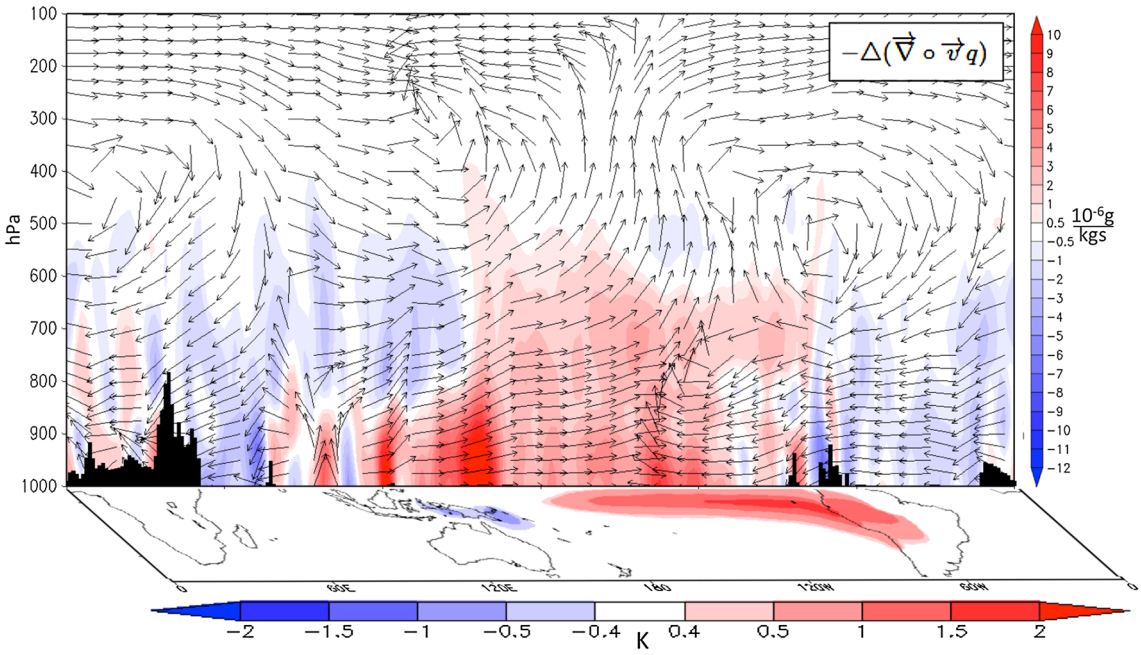

Fig. 14 Composite based on 7 warm Pacific summers in JRA reanalysis from 1961 to 2009 with JJAS Niño 3.4 index exceeding one standard deviation. The *upper panel* vectors show vertical and zonal wind speed anomalies averaged from 0 to 20 N. In the horizontal only every 5th vector is shown. *Colours* are the difference in horizontal moisture convergence in g/kgs on 27 pressure levels. The *lower panel* shows SST anomalies in Kelvin

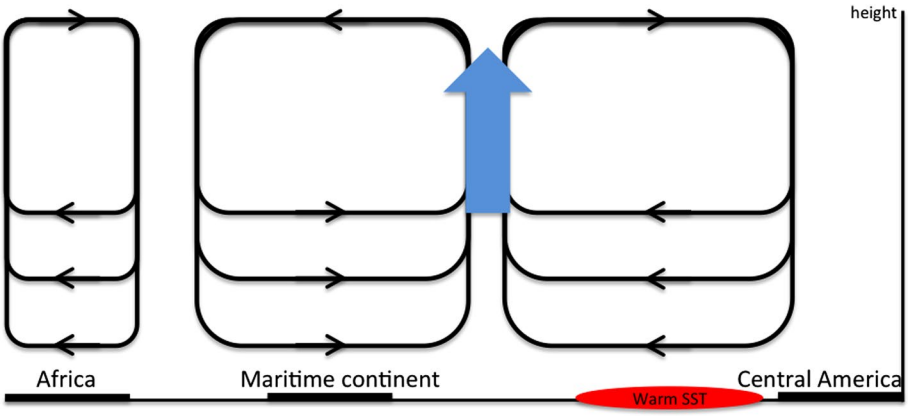

Fig. 15 Sketch of the large-scale circulation response to JJAS warm SST anomalies in the equatorial east Pacific, leading to a drying over East Africa

reproduces observed circulation changes in dry Ethiopian summers: the weakening of the Indian monsoon system with positive velocity potential anomalies in upper levels over the Indian Ocean and a weakening of the TEJ and the EALLJ. An additional sensitivity experiment confirms that the warm SST anomalies in the Pacific are the main factor driving the dry summers. While the convection over Ethiopia shows a positive response to the SST anomalies in the Pacific due to surface heating, the overall rainfall decreases.

The circulation response to the SST anomalies shows cell-like structures, which are sketched in Fig. 15. The upward motion over the west Pacific drives divergent flow at upper levels and convergent flow and sinking motion over the Indian Ocean.

We can confirm previous studies' findings of a weakened TEJ during dry Ethiopian summers. However, the conclusion of a weakened TEJ inducing sinking motion over Ethiopia is not as obvious. Our experiment shows overall local sinking anomalies with some shallow upward anomalies over the Ethiopian highlands, related to surface heating. This induces an overall decrease in large-scale rainfall, which dominates over a slight increase in local convective rainfall. However, vertical motion might not explain the suppression of rainfall in the experiment alone. The lower branch of the weakened

monsoon circulation over Africa, namely the easterly anomalies from the surface into the mid-troposphere, may contribute to a drying of the Ethiopian highlands. Such a weakening of the moisture transport into the region from the east in lower levels, the moisture pathways from the Indian Ocean and central Africa, has been observed in dry summer months (Viste and Sorteberg 2013).

Our results suggest that Kiremt rainfall deficits during developing El Niños are strongly controlled by upper-level circulation changes. Our model and experimental design suffers from some deficiencies that could affect our results: The large-scale circulation biases, that may overemphasize the importance of large-scale subsidence over Ethiopia, and the incorrect surface heat fluxes over the Indian Ocean arising from the prescribed SST (Copsey et al. 2006; Kucharski et al. 2007). These may explain the model's underestimation of the relative importance of central Pacific SST on Ethiopian rainfall. An intermodel-comparison and testing of different convection schemes is necessary to ensure the consistency of this mechanism and could possibly explain weaknesses of dynamical models to forecast Kiremt rainfall. Identifying the flaws of prediction systems may help to improve seasonal forecasts of Kiremt rainfall.

Acknowledgements We thank two anonymous reviewers and Dr. Teferi Demissie for their insightful comments. We also thank NMA for providing data and hosting a research stay. SG was supported by a fellowship from the University of Bergen and the Center for Climate Dynamics (SKD). The work was also supported by the European Union Seventh Framework Programme (FP7/2007-2013) PREFACE (Grant Agreements No. 603521), ERC STERCP project (Grant Agreement No. 648982), and from Research Council of Norway (233680/E10). Computing resources were provided by the Norwegian Program for supercomputing (NN9207k, NS9207k, NN9039K, NS9039K).

References

Äthiopien - Wirtschaft. Auswärtiges Amt - Deutschland. Accessed Sept 2015

Beltrando G, Camberlin P (1993) Interannual variability of rainfall in the eastern horn of Africa and indicators of atmospheric circulation. Int J Climatol 13:533–546. doi:10.1002/joc.3370130505

Berhane F, Zaitchik B, Dezfuli A (2013) Subseasonal analysis of precipitation variability in the Blue Nile River Basin. J Clim 27:325–344. doi:10.1175/JCLI-D-13-00094.1

Camberlin P (1997) Rainfall anomalies in the source region of the Nile and their connection with the Indian summer monsoon. J Clim 10:1380–1392. doi:10.1175/1520-0442(1997)010<1380:RAITSR>2.0.CO;2

Camberlin P (2009) Nile basin climates. In: Dumont H (ed) The Nile, vol 89., Monographiae BiologicaeSpringer, Dordrecht, pp 307–333. doi:10.1007/978-1-4020-9726-3_16

Camberlin P, Philippon N (2002) The East African march–may rainy season: associated atmospheric dynamics and predictability over the 1968–97 period. J Clim 15:1002–1019. doi:10.1175/1520-0442(2002)015<1002:TEAMMR>2.0.CO;2

Chakraborty A, Behera SK, Mujumdar M, Ohba R, Yamagata T (2006) Diagnosis of tropospheric moisture over Saudi Arabia and influences of IOD and ENSO. Mon Weather Rev 134:598–617. doi:10.1175/MWR3085.1

Copsey D, Sutton R, Knight JR (2006) Recent trends in sea level pressure in the Indian Ocean region. Geophys Res Lett. doi:10.1029/2006GL027175

Dinku T, Hailemariam K, Maidment R, Tarnavsky E, Connor S (2014) Combined use of satellite estimates and rain gauge observations to generate high-quality historical rainfall time series over Ethiopia. Int J Climatol 34:2489–2504. doi:10.1002/joc.3855

Diro GT, Black E, Grimes DIF (2008) Seasonal forecasting of Ethiopian spring rains. Meteorol Appl 15:73–83. doi:10.1002/met.63

Diro GT, Grimes DIF, Black E (2011a) Large scale features affecting Ethiopian rainfall. In: Williams CJR, Kniveton DR (eds) African climate and climate change, vol 43., Advances in global change researchSpringer, Netherlands, pp 13–50

Diro GT, Grimes DIF, Black E (2011b) Teleconnections between Ethiopian summer rainfall and sea surface temperature: part I—observation and modelling. Clim Dyn 37:103–119. doi:10.1007/s00382-010-0837-8

Diro GT, Toniazzo T, Shaffrey L (2011c) Ethiopian Rainfall in Climate Models. In: Williams RCJ, Kniveton RD (eds) African climate and climate change: physical, social and political perspectives. Springer, Dordrecht, pp 51–69. doi:10.1007/978-90-481-3842-5_3

Gissila T, Black E, Grimes DIF, Slingo JM (2004) Seasonal forecasting of the Ethiopian summer rains. Int J Climatol 24:1345–1358. doi:10.1002/joc.1078

Gleixner S, Keenlyside N, Hodges KI, Tseng W-L, Bengtsson L (2014) An inter-hemispheric comparison of the tropical storm response to global warming. Clim Dyn 42:2147–2157. doi:10.1007/s00382-013-1914-6

Griffiths JF (1972) Ethiopian highlands. In: World survey of climatology, vol 10. Elsevier, Amsterdam. ISBN:0444408932

Hansen JW, Mason SJ, Sun L, Tall A (2011) Review of seasonal climate forecasting for agriculture in Sub-Saharan Africa. Exp Agric 47:205–240. doi:10.1017/S0014479710000876

Holton JR, Hakim GJ (2013) Chapter 10—the general circulation. In: Holton JR, Hakim GJ (eds) An introduction to dynamic meteorology, 5th edn. Academic Press, Boston, pp 325–375

Jiang X et al (2015) Vertical structure and physical processes of the Madden–Julian oscillation: exploring key model physics in climate simulations. J Geophys Res Atmos 120:4718–4748. doi:10.1002/2014JD022375

Kobayashi S et al (2015) The JRA-55 reanalysis: general specifications and basic characteristics. J Meteorol Soc Jpn 93:5–48. doi:10.2151/jmsj.2015-001

Korecha D, Barnston AG (2007) Predictability of June–September rainfall in Ethiopia. Mon Weather Rev 135:628–650. doi:10.1175/MWR3304.1

Korecha D, Sorteberg A (2013a) Construction of homogeneous rainfall regimes for Ethiopia. Submitted to Int J Climatol

Korecha D, Sorteberg A (2013b) Validation of operational seasonal rainfall forecast in Ethiopia. Water Resour Res 49:7681–7697. doi:10.1002/2013wr013760

Kucharski F, Bracco A, Yoo JH, Molteni F (2007) Low-frequency variability of the Indian monsoon–ENSO relationship and the

tropical Atlantic: the "weakening" of the 1980s and 1990s. J Clim 20:4255–4266. doi:10.1175/JCLI4254.1

Maidment RI et al (2014) The 30 year TAMSAT African rainfall climatology and time series (TARCAT) data set. J Geophys Res Atmos 119:10619–10644. doi:10.1002/2014jd021927

Mohamed YA, van den Hurk BJJM, Savenije HHG, Bastiaanssen WGM (2005) Hydroclimatology of the Nile: results from a regional climate model. Hydrol Earth Syst Sci 9:263–278. doi:10.5194/hess-9-263-2005

Mohino E et al (2011) Changes in the interannual SST-forced signals on West African rainfall. AGCM intercomparison. Clim Dyn 37:1707–1725. doi:10.1007/s00382-011-1093-2

Mutai CC, Ward MN, Colman AW (1998) Towards the prediction of the East Africa short rains based on sea-surface temperature-atmosphere coupling. Int J Climatol 18:975–997. doi:10.1002/(sici)1097-0088(199807)18:9<975:aid-joc259>3.3.co;2-l

Otieno V, Anyah R (2013) CMIP5 simulated climate conditions of the Greater Horn of Africa (GHA). Part 1: contemporary climate. Clim Dyn 41:2081–2097. doi:10.1007/s00382-012-1549-z

Peixoto JP (1992) Physics of climate. Melville, American Institute of Physics New York

Roeckner E et al (2003) The atmospheric general circulation model ECHAM 5. Part I. Model description. Max-Planck-Institute for Meteorology, Hamburg

Sperber KR et al (2013) The Asian summer monsoon: an intercomparison of CMIP5 vs. CMIP3 simulations of the late 20th century. Clim Dyn 41:2711–2744. doi:10.1007/s00382-012-1607-6

Segele ZT, Lamb PJ (2005) Characterization and variability of Kiremt rainy season over Ethiopia. Meteorol Atmos Phys 89:153–180

Segele ZT, Lamb PJ, Leslie LM (2009a) Large-scale atmospheric circulation and global sea surface temperature associations with Horn of Africa June–September rainfall. Int J Climatol 29:1075–1100

Segele ZT, Leslie LM, Lamb PJ (2009b) Evaluation and adaptation of a regional climate model for the Horn of Africa: rainfall climatology and interannual variability. Int J Climatol 29:47–65. doi:10.1002/joc.1681

Segele ZT, Leslie LM, Tarhule A (2015) Sensitivity of horn of Africa rainfall to regional sea surface temperature forcing. J Clim 3:365

Seleshi Y, Demaree GR (1995) Rainfall variability in the Ethiopian and Eritrean highlands and its links with the southern oscillation index. J Biogeogr 22:945–952. doi:10.2307/2845995

Shaman J, Tziperman E (2007) Summertime ENSO–North African-Asian Jet teleconnection and implications for the Indian monsoons. Geophys Res Lett. doi:10.1029/2006GL029143

Smith TM, Reynolds RW, Peterson TC, Lawrimore J (2008) Improvements to NOAA's historical merged land–ocean surface temperature analysis (1880–2006). J Clim 21:2283–2296. doi:10.1175/2007JCLI2100.1

Tiedtke M (1996) An extension of cloud-radiation parameterization in the ECMWF model: the representation of subgrid-scale variations of optical depth. Mon Weather Rev 124:745–750. doi:10.1175/1520-0493(1996)124<0745:aeocrp>2.0.co;2

Tsegay W-G (1997) El Niño and drought early warning in Ethiopia. Internet J Afr Stud 2. Available at http://www.bradford.ac.uk/researchold/ijas/ijasno2/Georgis.html

Tseng W-L (2012) Role of ocean-atmosphere interaction for tropical climate variability over warm pool regions. Doctoral Thesis, Christian-Albrechts-Universität Kiel

Viste E, Sorteberg A (2013) The effect of moisture transport variability on Ethiopian summer precipitation. Int J Climatol 33:3106–3123

Viste E, Korecha D, Sorteberg A (2013) Recent drought and precipitation tendencies in Ethiopia. Theor Appl Climatol 112:535–551. doi:10.1007/s00704-012-0746-3

Von Storch H, Zwiers FW (2001) Statistical analysis in climate research. Cambridge University Press, Cambridge